Author/s:
Seyer, B;Diwakarla, S;Burns, P;Hallberg, A;Grönbladh, A;Hallberg, M;Chai, SY

Title:
Insulin-regulated aminopeptidase inhibitor-mediated increases in dendritic spine density are facilitated by glucose uptake

Date:
2020-05-01

Citation:
Seyer, B., Diwakarla, S., Burns, P., Hallberg, A., Grönbladh, A., Hallberg, M. & Chai, S. Y. (2020). Insulin-regulated aminopeptidase inhibitor-mediated increases in dendritic spine density are facilitated by glucose uptake. Journal of Neurochemistry, 153 (4), pp.485-494. https://doi.org/10.1111/jnc.14880.

DR. SHANTI DIWAKARLA (Orcid ID : 0000-0003-2328-3528)

Article type : Original Article

Insulin-regulated aminopeptidase inhibitor-mediated increases in dendritic spine density are facilitated by glucose uptake

Benjamin Seyer[1,*], Shanti Diwakarla[2,4,*], Peta Burns[1], Anders Hallberg[3], Alfhild Grönbladh[2], Mathias Hallberg[2], and Siew Yeen Chai[1]

[1]Biomedicine Discovery Institute, Department of Physiology, Faculty of Biomedical and Psychological Sciences, Monash University, Clayton, VIC 3800, Australia.
[2]The Beijer Laboratory, Department of Pharmaceutical Biosciences, Division of Biological Research on Drug Dependence, Uppsala University, BMC, SE-751 24 Uppsala, Sweden.
[3]Department of Medicinal Chemistry, Uppsala University, BMC, SE-751 23 Uppsala, Sweden.

[*]These authors contributed equally to this work

[4]Current address:
Florey Institute of Neuroscience and Mental Health, Parkville, VIC, 3050, Australia.

Running Title: IRAP inhibition increases dendritic spine density

Keywords: IRAP, memory, glucose uptake, dendritic spines, hippocampal neurons, spine morphology

Abbreviations: Ang IV, Angiotensin IV; DAPI, 4',6-diamidino-2-phenylindole dihydrochloride; DMSO, dimethyl sulfoxide; DSD, dendritic spine density; $GLUT_4$, glucose transporter 4; IRAP, insulin-regulated aminopeptidase; LVV-H7, LVV hemorphin 7; MMPs, matrix-metalloproteases; RRID, Research Resource Identifier (see scicrunch.org); SAT, spontaneous alternation task; vGlut1, vesicular glutamate transporter 1.

Corresponding Author:

A/Prof Siew Yeen Chai

Biomedicine Discovery Institute, Department of Physiology, Faculty of Biomedical and Psychological Sciences, Monash University, Clayton, VIC 3800, Australia

Email: siew.chai@monash.edu

Tel: +61 3 990 52515

Fax: +61 3 990 52547

Abstract

Ethyl 2-acetylamino-7-hydroxy-4-pyridin-3-yl-4H-chromene-3-carboxylate (HFI-419), the benzopyran-based inhibitor of insulin-regulated aminopeptidase (IRAP), has previously been shown to improve spatial working and recognition memory in rodents. However, the mechanism of its cognitive-enhancing effect remains unknown. There is a close correlation between dendritic spine density and learning *in vivo* and several studies suggest that increases in neuronal glucose uptake and/or alterations to the activity of matrix metalloproteinases (MMPs) may improve memory and increase dendritic spine density. We aimed to identify the potential mechanism by which HFI-419 enhances memory by utilizing rat primary cultures of hippocampal cells. Alterations to dendritic spine density were assessed in the presence of varying concentrations of HFI-419 at different stages of hippocampal cell development. In addition, glucose uptake and changes to spine density were assessed in the presence of indinavir, an inhibitor of the glucose transporter 4 ($GLUT_4$), or the matrix metalloprotease inhibitor CAS 204140-01-2. We confirmed that inhibition of IRAP activity with HFI-419 enhanced spatial working memory in rats, and determined that this enhancement may be driven by $GLUT_4$-mediated changes to dendritic spine density. We observed that IRAP inhibition increased dendritic spine density prior to peak dendritic growth in hippocampal neurons, and that spine formation was inhibited when $GLUT_4$-mediated glucose uptake was blocked. In addition, during the peak phase of dendritic spine growth, the effect of IRAP inhibition on enhancement of dendritic spine density resulted specifically in an increase in the proportion of mushroom/stubby-like spines, a morphology associated with memory and learning. Moreover, these spines were deemed to be functional based on their expression of the presynaptic markers vesicular glutamate transporter 1 and synapsin. Overall, or findings suggest that IRAP inhibitors may facilitate memory by increasing hippocampal dendritic spine density via a $GLUT_4$-mediated mechanism.

Introduction

The effect of insulin-regulated aminopeptidase (IRAP) inhibition on cognitive enhancement is well-documented. The peptide inhibitors of IRAP, angiotensin IV (Ang IV) and LVV hemorphin 7 (LVV-H7), have been shown to improve memory across a variety of behavioral paradigms including passive avoidance tasks (Braszko *et al.* 1988, Braszko *et al.* 1991, Wright *et al.* 1993) and spatial navigation tasks such as the Morris water maze (Wright *et al.* 1999a, Wright *et al.* 1999b) and Barnes circular maze (Lee *et al.* 2004). Furthermore, peptide IRAP inhibitors are able to improve cognitive function in rodents subjected to chronic alcohol exposure (Wisniewski *et al.* 1993), global ischemia (Wright *et al.* 1996), bilateral perforant pathway lesions (Wright et al. 1999a), and disruptions to the septo-hippocampal cholinergic pathway (Pederson *et al.* 2001, Lee et al. 2004, Olson & Cero 2010, Olson *et al.* 2004). While promising, peptide inhibitors of IRAP are unsuitable in a clinical setting due to off-target effects, rapid degradation, and poor blood-brain-barrier permeability. At micromolar concentrations, Ang IV has also been shown to bind to the angiotensin II receptor type 1 (AT1), the angiotensin II receptor type 2 (AT2) (Bosnyak *et al.* 2011, Hallberg *et al.* 2017), and inhibit aminopeptidase N (Lantz *et al.* 1991, Fruitier-Arnaudin *et al.* 2002, Garreau *et al.* 1998), and LVV-H7 to the μ-opioid receptor (Nyberg *et al.* 1996).

A small molecule benzopyran-based IRAP inhibitor with nanomolar affinity (K_i = 420 nM), ethyl 2-acetylamino-7-hydroxy-4-pyridin-3-yl-4H-chromene-3-carboxylate (HFI-419), has previously been shown to have a cognitive enhancing effect in rodents similar to that seen with the peptide inhibitors Ang IV and LVV-H7 (Albiston *et al.* 2008, De Bundel *et al.* 2009). However, the mechanisms by which HFI-419 exerts its effects remain unclear. Two likely mechanisms by which inhibition of IRAP leads to enhancement of memory are an increase in neuronal glucose uptake or an increase in the activity of matrix-metalloproteases (MMPs), where modulation of both systems are known to improve memory and learning as well as affect dendritic spine density (DSD). Dendritic spines are small protrusions from the dendrites of neurons that serve as contacts with neighboring

axons and contain all of the molecular machinery required for synaptic plasticity and long term potentiation, i.e. the storage of memories. There is a close correlation between DSD and learning *in vivo* that has been demonstrated in a number of behavioral studies such as passive avoidance (O'Malley *et al.* 1998), water maze tasks (Moser *et al.* 1994, O'Malley *et al.* 2000), fear conditioning (Lai *et al.* 2012), and repetitive motor tasks (Fu *et al.* 2012).

Increased glucose uptake in neurons is known to occur following IRAP inhibitor treatment (Fernando et al, 2008) (Albiston et al. 2008) and glucose loading has been demonstrated to enhance cognition (Lee *et al.* 1988, Smith *et al.* 2011). Furthermore, glucose can activate mammalian target of rapamycin, which in turn can alter DSD (Dash *et al.* 2006). Interestingly, observations from our collaborators (Lee, submitted manuscript) have noted that IRAP inhibition reduces the activity of tissue inhibitor of metalloproteinases-1, an inhibitor of the MMP system. In turn, the activity of MMPs is important for degradation of the extracellular matrix, a crucial step in allowing the growth of dendritic spines.

In addition to HFI-419, the development of several other families of nonpeptide IRAP inhibitors have been reported including peptidomimetics and small molecular weight compounds. Macrocyclic and arylsulfonamide derived IRAP inhibitors have already been demonstrated to enhance DSD in primary hippocampal cell cultures (Diwakarla *et al.* 2016a, Diwakarla *et al.* 2016b), however these new classes of inhibitors are yet to be tested *in vivo* for their memory enhancing ability.

Given that HFI-419 has been demonstrated to facilitate memory and learning *in vivo*, we aimed to determine its potential mechanism of action using primary cultures of hippocampal neurons, which would allow a thorough analysis of changes in DSD and correlations to be drawn with alterations in glucose uptake and inhibition of MMPs. We also confirmed the memory enhancing effects of HFI-419 following central administration in rats using the spontaneous alternation task, a test of spatial working memory.

Methods

Animals

For the *in vivo* experiments, male Sprague Dawley rats (270 – 310g, 7 – 8 weeks old, n=16) were housed in groups of 4, in open top cages, with free access to standard rat chow and water until the time of surgery (at least 1 week acclimatization period). All experiments were approved by the Monash University Animal Welfare Committee under the Monash Animal Research Platform 2011/117 application and performed according to the National Health and Medical Research Council of Australia "Code of practice for the care and use of animals for scientific purposes". For the *in vitro* studies, pregnant Sprague-Dawley rats (Charles River, Sulzfeld, Germany or ARC, WA, Australia; RRID: RGD_10395233) were used for the isolation of hippocampal neurons from embryonic day 17

fetuses of mixed sex. All studies were approved by the Uppsala Animal Care and Ethical Committee under (C15/14) or the Monash University Animal Ethics Committee, and followed the guidelines of the Swedish legislation on animal experimentation or the Australian National Health and Medical Research Council code of practice for the care and use of animals for scientific purposes. This exploratory study was not pre-registered.

Intracerebroventricular Surgery and the Spontaneous Alternation Task

A total of 16 rats were anaesthetized with 5% (v/v) isoflurane (Cat # FGISO0250 (2014), Pharmachem, Queensland, Australia) in 100% oxygen (1 L/min, Cat # 400 (2014), BOC, Victoria, Australia) for approximately 1-2 min before being placed in a stereotaxic frame, where anesthesia was maintained at 3% (v/v) isoflurane in 100% oxygen (1 L/min) through a nose cone to minimize animal suffering during the procedure. Depth of anesthesia was ensured by paw-pinch response to pain. Rats were implanted with an indwelling cannula (22 gauge; Cat # C313GA/SPC (2014), Plastics One, VA, USA) in the right cerebral ventricle using the following flat skull coordinates; 0.8 mm posterior to Bregma, 1.5 mm lateral to the midline and 3.5 mm ventral to the surface of the skull. The cannula was secured to the skull with a stainless steel screw and dental cement. During brain collection it was confirmed that the screw did not penetrate the dura. Meloxicam (1 mg/kg; Ilium, Cat # 3465 (2013), Troy Laboratories, NSW, Australia) was administered subcutaneously during surgery and rats were supplied with 15 mL of 200 mg/kg paracetamol in 10% (w/v) sugar water for two nights post-surgery as analgesia. Surgeries took place between 9-12am.

Correct cannula placement was confirmed by observing a dipsogenic response to angiotensin II (Cat # 2078 (2014), Auspep, Melbourne, Australia) Five days post-surgery rats received an injection into the lateral ventricle of 2 µL of 25 nM of Angiotensin II and were placed back in their home cage. Water intake was measured every 5 minutes for 20 minutes. Rats that drank a minimum of 5 mL in the first 15 min were included in the study. No animals consumed less than 5 mL of water in the first 15 min following Angiotensin II administration. Therefore, no animals were excluded from this study. Testing was performed between 10-12am.

The spontaneous alternation in the plus maze task (SAT) was used to measure spatial working memory in vehicle- and HFI-419-treated rats according to a previously described method (Albiston et al. 2008). Testing was performed during the light phase (resting phase) between 9-12am (Figure 1). The plus maze had four arms measuring 75 (long) × 10 (wide) × 20 (high) cm and visual cues placed 1 m away from the center of the maze. Prior to each behavioral task, the rats were acclimatized to the testing room for 40 minutes. No randomization was performed to allocate rats in the study and HFI-419-treated rats were assessed before vehicle-treated rats. Rats were injected with 0.1 nM HFI-419 in 2 µL of 10% (v/v) dimethyl sulfoxide (DMSO, Cat # 317275 (2013), Merck Millipore, Melbourne, Australia) or vehicle (10% (v/v) DMSO). After 5 min, animals were placed in the center of the maze

(all animals were placed facing the same arm) and allowed to explore the apparatus for 20 minutes. The testing apparatus was sprayed and wiped down with 80% (v/v) ethanol at the beginning of each behavioural experiment to remove olfactory cues. The number and sequence of arm entries was recorded for calculation of a percent alternation score. Alternation scoring was performed by a researcher blinded to the treatment groups. An alternation consisted of 4 different arm choices over 5 consecutive arm entries. Dividing the number of observed alternations in overlapping quintuplets by the number of possible alternations and multiplying the quotient by 100 calculated an alternation score.

Following behavioural testing (3 days post behaviour), rats were anaesthetized by intraperitoneal injection of sodium pentobarbital (20 mg/kg) before being transcardially perfused with ice-cold phosphate buffered saline (PBS; pH 7.3) and then ice-cold 4% (w/v) paraformaldehyde (Cat # 158127 (2014), Sigma-Aldrich, St. Louis, MO) in PBS. The tissue collected was not used for the current study.

Primary Hippocampal Cultures

Early spine formation: All measures were taken to minimize pain and suffering of the experimental animals. Pregnant Sprague Dawley rats were anesthetized at E17 with 5% (v/v) isoflurane (1 L/min oxygen) until disappearance of pain reflexes (paw-pinch) and killed by cervical dislocation. Primary hippocampal cultures were prepared from embryonic day 17 rat fetuses as previously described (Diwakarla et al. 2016a). One pregnant dam was used for each culture. The hippocampi from all embryos were isolated and pooled. Hippocampi were chemically and mechanically digested using trypsin and trituration with a 1 ml pipette, respectively, and seeded on poly-D-lysine coated glass coverslips (50 µg/mL, Cat # P0899 (2015), Sigma-Aldrich) in 24-well plates at a density of 1×10^5 cells per well, and maintained in neurobasal medium (Cat # 21103049 (2015), Invitrogen, Carlsbad, CA) supplemented with B27 (Cat #. 17504-044 (2015), Invitrogen), 0.5 mM GlutaMAX supplement (Cat # 35050-061 (2015), Invitrogen). Cultures were grown in the presence of 10% (v/v) fetal bovine serum (Cat # 10099-141 (2015), Invitrogen;) for the first 24 h, after which the media was replaced with serum-free Neurobasal medium supplemented with 2% (v/v) extra B27. Cultures were maintained at 37°C/5% (v/v) CO_2 in a humidified incubator and partial media changes were performed twice a week. To determine if HFI-419 could enhance total spine formation prior to peak dendritic spine growth, cells were exposed to varying concentrations of HFI-419 at 8, 11 and 14 div. Treatments were ceased at 15 div. To investigate the influence of glucose uptake and MMP activation, cells were either treated in the presence or absence of the highly selective glucose transporter 4 ($GLUT_4$) inhibitor indinavir (50 µM; Cat # SML0189 (2015), Sigma-Aldrich) or the MMP-9/MMP-13 inhibitor I, CAS 204140-01-2 (100 and 200 µM; Cat # 444252 (2015), Merck Millipore). All treatments were performed at 8, 11 and 14 div.

Peak spine formation and classification of spines: Primary hippocampal cultures were prepared as described above. To determine the effect of HFI-419 on peak spine formation and conduct a thorough investigation on their morphology (i.e. mushroom/stubby vs. filopodia/thin spines) and functionality, cells were grown for 13 days *in vitro* (div) and the addition of varying concentrations of HFI-419 or vehicle (0.1% (v/v) (DMSO)) was performed on day 14, 17, and 20 div. Treatments were ceased at 21 div. Brain-derived neurotrophic factor (BDNF; 100 ng/ml; Cat # 242-BDB (2015), R&D Systems, MN, USA) was used as a positive control for enhanced spine formation (Alonso *et al.* 2004).

Immunohistochemistry and quantification of dendritic spines

Immunocytochemistry and analysis of dendritic spine density and functionality were performed as previously described (Diwakarla et al. 2016a). At 15 (early spine formation) or 21 div (peak spine formation), cells were fixed, blocked with phosphate buffered saline (PBS) containing 10% (v/v) normal donkey serum (Cat # D9663 (2014), Sigma Aldrich) and 0.1% (v/v) Triton-X-100 (Cat # T8787 (2014), Sigma-Aldrich), and stained for the neuronal marker rabbit anti-β III-tubulin antibody (1:500; RRID: AB_262133, Sigma-Aldrich) and the dendritic spine marker mouse anti-drebrin antibody (1:500; RRID: AB_10621721, Enzo Life Sciences, Farmingdale, NY) for 90 min at room temperature. For spine functionality experiments, cells were double labeled with drebrin and the presynaptic glutamatergic synapse marker rabbit anti-vesicular glutamate transporter 1 antibody (vGlut1; 1:500; RRID: AB_10710315, Abcam, Cambridge, MA) or drebrin and the universal presynaptic marker rabbit anti-synapsin1 antibody (1:500; RRID: AB_2200097, Abcam). Cells were incubated for 1 h at room temperature with the appropriate fluorescent-conjugated secondary antibodies (1:500; Alexa 488 and Alexa 568; RRID: AB_141708, AB_2534013, AB_141607, Invitrogen) and washed 3 times with PBS before being counterstained with 4',6-diamidino-2-phenylindole dihydrochloride (DAPI; Cat # 268298 (2015), Merck Millipore) and mounted with MOWIOL anti-fade mounting medium (Cat # 475904 (2015), Sigma-Aldrich).

Microscope slides were relabeled by another researcher so that the experimenter was blinded to the treatment groups. Single images were captured using a Zeiss LSM700 inverted confocal microscope (Carl Zeiss Microscopy GmbH, Jena, Germany) with a ×63 oil immersion lens. Stubby/mushroom-like spines and filopodia/thin-like spines were identified and counted as previously described (Diwakarla et al. 2016a). Spines staining positive for drebrin, vGlut1, or synapsin1 were counted on three individual basal dendrites (primary and secondary) from 10 neurons per culture (i.e. 30 dendrites from 3 independent cell culture preparations) using Image J 1.49e software (National Institutes of Health, Bethesda, MD; RRID:SCR_003070). Quantification was performed on 50 µm dendritic segments that were at least 50 µm away from the cell body. The number of spines counted for each dose was expressed as a percentage of the vehicle control for each independent culture to

account for any variation between cultures. To ensure specificity of labeling, immunostaining was performed where the primary antibodies were omitted as a negative control.

Glucose Uptake

Hippocampal neurons were treated with a single dose of HFI-419 in the preincubation buffer prior to the glucose uptake assay on day 15. To perform the assay, media was removed and replaced with glucose free neurobasal A medium (Cat # 10888022 (2014), Invitrogen), supplemented with 5 mM D-glucose and, in the case of the single treatment, the appropriate dose of HFI-419 was dissolved in 100% (v/v) DMSO (final DMSO concentration 0.1% (v/v)). Combinations of 40 mM potassium, to stimulate cells (as the majority of IRAP and $GLUT_4$ are sequestered intracellularly), and 50 μM indinavir, were also added. After 30 min, 1 μCi/mL 2-[1-14C]-Deoxy-D-glucose (Cat # NEC495A001MC (2014), PerkinElmer, WA, Australia) was added to cultures for an additional 30 min. Following this, the cells were washed with ice-cold phosphate buffered saline three times to stop uptake and to remove excess labelled glucose before the cells were lysed with 0.1% (v/v) Triton-X-100. Plates were then scraped and the lysates were added to 2 mL UltimaGold Scintillation buffer (Cat# 6013327 (2014), Perkin Elmer) before being counted in a TriCarb 2810 TR Liquid Scintillation Analyser (Perkin Elmer). No blinding was performed for this experiment.

Statistical Analysis

All data were tested for normality using the Shapiro–Wilk test. No tests were performed for outliers and no data were excluded from the analysis. Data were analyzed with Student's unpaired *t* test (glucose uptake, SAT, and neurotransmitter signature of spines) or one-way analysis of variance with Dunnett's *post hoc* analysis using GraphPad Prism, version 8 (GraphPad software Inc., San Diego, CA, USA; RRID: SCR_002798). Data are represented as the mean ± SEM. p values < 0.05 was considered statistically significant. Sample size was not predetermined by formal power statistical methods. There were no sample size differences between the beginning and end of the experiments. The sample number of each experiment is presented in the figures.

Results

IRAP inhibition with HFI-419 enhanced spatial working memory

The effect of centrally administered HFI-419 on memory was assessed using the SAT. In agreement with our previous study (Albiston et al. 2008) a significant treatment effect was observed in rats treated with HFI-419 compared with animals administered vehicle (Figure 2A; $p = 0.0256$). HFI-419-treated rats had improved spatial working memory as indicated by the higher alternation scores

when compared with vehicle controls. In addition, the number of total arm entries was recorded and was found to be the same between vehicle- and HFI-419- treated rats demonstrating no drug effect on locomotor activity and that the higher alternation scores are not due to increased activity (Figure 2B; p=0.9559).

HFI-419 increased dendritic spine density in hippocampal cultures and this process was mediated by $GLUT_4$.

According to Kaech and Banker, dendritic development, synaptogenesis and synaptic plasticity in hippocampal cultures occurs between 1 and 4 weeks in culture, with peak dendritic growth and synapse formation occurring during the second and third week (i.e. 14-21 div) (Kaech & Banker 2006). When cells were exposed to varying concentrations of HFI-419 at time points prior to peak dendritic growth and synapse formation (i.e. 8, 11, and 14 div), the increase in the number of spines was markedly visible (Figure 3A). When the total number of spines was quantified, a bell shaped dose response was observed, with a peak response at 10^{-6} M (1 μM) (Figure 3B; p=0.0132). These results indicate that HFI-419 can significantly enhance total spine formation at a time point prior to peak spine growth.

To investigate how HFI-419 may enhance spine growth, hippocampal cultures were co-treated with HFI-419 and indinavir, to block $GLUT_4$-mediated glucose uptake (Murata *et al.* 2002), or the MMP-9/MMP-13 inhibitor I, CAS 204140-01-2, to block MMPs (Cheng *et al.* 2000). Indinavir completely abolished the increase in dendritic spine growth induced by HFI-419 treatment (Figure 4; p=0.0114) indicating the importance of glucose uptake in driving increased DSD. Interestingly, neither dose of the MMP-9/MMP-13 inhibitor I (100μM or 200 μM) affected the increase in dendritic spine density induced by HFI-419 treatment.

HFI-419 increased glucose uptake in cultured hippocampal neurons.

Glucose is known to play an important role in the formation and enhancement of hippocampal dendritic spines (Mainardi *et al.* 2015). The reduction of dendritic spine density following IRAP inhibitor treatment in the presence of indinavir indicated that $GLUT_4$ (and thus glucose uptake) played an important role in enhancing dendritic spine formation. Hippocampal cells that were treated with HFI-419 prior to the glucose uptake assay produced a bell-shaped dose-response with the same effective dose as seen in the spine density assay (Figure 5A; p=0.0200). In order to confirm that the increase in glucose uptake was mediated by $GLUT_4$, the cultures were also co-treated with indinavir (50 μM), which resulted in a significant reduction in HFI-419-mediated glucose uptake (Figure 5B; p=0.0438). Interestingly, K^+ had no effect on glucose uptake (p=0.9997), however, this may be due to the already stimulated state of cells caused by the culture conditions.

Inhibition of IRAP activity with HFI-419 enhanced the proportion of mushroom/stubby spines.

To determine if HFI-419 could enhance DSD during a the peak phase of dendritic growth and spine formation, cells were treated with HFI-419 at 14, 17, and 20 div. Similar to early hippocampal cultures, an increase in dendritic spine densities was observed in response to HFI-419 treatment when compared to vehicle-treated cells at this peak phase of dendritic growth (Figure 6A). This increase in dendritic spine density was similar to that seen with BDNF, a known enhancer of spine formation (Alonso *et al.* 2004).

To further understand the precise effect HFI-419 was having on dendritic spine formation at this timepoint in hippocampal growth, the spines were further classified based on their morphology. Similar to early treatment of cultures, HFI-419, at 10^{-6} M (1 μM), induced a significant increase in the densities of dendritic spine (Figure 6B; p=0.0271), albeit to a lesser extent. In addition, treatment with 10^{-6}M (1 μM) HFI-419 stimulated a significant increase in mushroom spine density (p=0.0134, 27% increase), this spine morphology is generally associated with the storage of information (Figure 6C). No change was observed for filopodia/thin spines (Figure 6D), a morphology typically associated with immature spine.

HFI-419 increased the number of functional dendritic spines.

To determine whether the newly developed mushroom spines were functional and capable of excitatory neurotransmission, immunohistochemical staining against the presynaptic markers synapsin1, a universal marker of synaptic terminals, and vGLUT1, a marker of glutamatergic synapses, was performed on cells exposed to 10^{-6}M (1 μM) HFI-419. Immunohistochemical analysis revealed that there was a significant increase in the number of synapsin1-positive (Figure 7A; p=0.0129) and vGLUT1-positive (Figure 7B; *p=0.0088*) mushroom/stubby spines when compared with vehicle, once again indicating that 10^{-6}M (1 μM) HFI-419 can increase DSD. However, because the total number of spines also increased, the ratio of synapsin1- and vGLUT1-positive mushroom/stubby spines did not differ from vehicle treated cells (>80%), indicating that the proportion of functional spines remained the same (Figure 6C and 6D, p=0.7972 and p=0.3676, respectively). These results indicate that HFI-419 not only increases the number of total spines, they demonstrate that these spines are functional and are capable of neurotransmission. As observed in vehicle-treated cells, there were fewer vGLUT1-positive spines compared with synapsin1-positive spines, suggesting that some synapses act independently of glutamate signaling and may interact with cholinergic or GABAergic neurons. Overall, these data indicate that cells treated with 10^{-6} M (1 μM) HFI-419 have the capacity to receive increased excitatory synaptic input, which plays an important role in the process of memory and learning.

Discussion

The aim of this study was to understand the potential mechanism behind the memory-enhancing effect of the IRAP inhibitor HFI-419. We sought to first confirm the cognitive enhancing potential of the IRAP inhibitor and use two *in vitro* bioassays to investigate the effect IRAP inhibition exerts in primary cultures of hippocampal neurons.

HFI-419 has previously been shown to enhance both spatial working and recognition memory measured by spontaneous alternation in the plus maze and in the novel object recognition tasks, respectively (Albiston et al. 2008). Despite these promising results, the specific mechanism by which the IRAP inhibitor exerts its beneficial effects on cognition is still unknown. Dendritic spines are small protrusions that are located on the dendrites of neurons. In order to respond to novel inputs, spines must be highly plastic and able to modulate their shape and signal rapidly. Spines come in various shapes, but the two most relevant to memory are the thin and mushroom spines. Biochemically, thin spines have small post-synaptic densities and contain a high proportion of NMDA receptors. On stimulation of the spines, these receptors cause an influx of calcium, which triggers a cascade of intracellular signaling leading to the eventual insertion of AMPA receptors into the plasma membrane at the post-synaptic density. To accommodate these extra receptors, the postsynaptic density must grow in size and with it the spine head, leading to the transition from thin to mushroom.

We initially investigated the effect of HFI-419 in hippocampal neurons that had not undergone the peak phase of spine growth. HFI-419 had a significant effect on total spine formation, and demonstrated a dose-dependent effect, with the most effective dose being 1 μM. This bell-shaped dose response curve has been observed for macrocyclic and arylsulfonamide classes of IRAP inhibitors (Diwakarla et al. 2016a, Diwakarla et al. 2016b), as well as the peptide inhibitor Ang IV (Benoist *et al.* 2011).

Several lines of evidence have shown the close relationship between IRAP and $GLUT_4$ (Albiston et al. 2008, Fernando *et al.* 2008, Jiang *et al.* 2001) in particular, their colocalization in the pyramidal neurons in the hippocampus (Fernando et al. 2008). In adipocytes and skeletal muscles, IRAP is thought to play a role in regulating the trafficking of $GLUT_4$ (Keller *et al.* 2002). In hippocampal neurons, depolarization of the plasma membrane resulted in $GLUT_4$-mediated glucose uptake that was enhanced by IRAP inhibitor treatment (Fernando et al. 2008). Since exogenous glucose administration has been shown to facilitate memory and learning, a potential mechanism by which IRAP inhibition enhances spatial working memory could be via increased glucose uptake into neurons. In this study, inhibition of $GLUT_4$-mediated glucose uptake by indinavir abolished spine growth that was induced by IRAP inhibitor HFI419 treatment. The effect of HFI-419 on glucose uptake demonstrated a bell-shaped dose response with peak efficacy matching that of the effect of the

drug on dendritic spine density. The reduction in dendritic spine number with co-treatment with indinavir combined with the similar dose-response for the IRAP inhibitor on glucose uptake suggests that HFI-419 may cause an increase in DSD through an increase in $GLUT_4$-mediated glucose uptake. Although this study specifically focused on the effect of HFI-419 on spine density and glucose uptake, it should be noted that indinavir treatment alone may also affect spine density, with a previous study showing that indinavir can reduce basal levels of glucose in L6 myoblasts (Rudich *et al.* 2003).

IRAP inhibition was able to increase total DSD in hippocampal cultures undergoing peak dendritic spine growth as was observed when HFI-419 was administered to cells at earlier div. The most effective dose was observed to be 10^{-6} M (1 μM). Further analysis revealed that HFI-419 treatment increased the number of mushroom spines, but had little effect on the number of filopodia-like/thin spines. This result suggests that IRAP inhibition may act by modulating the activity of the NMDA receptors to change the morphology of the spine head, however further studies are needed to confirm this. In addition to increasing the number of total dendritic spines, HFI-419 increased the number of functional spines, as assessed by synapsin1 and vGLUT1 staining. Synapsin1 is required for maintaining vesicles at excitatory synapses (Gitler *et al.* 2004) while the presence of vGLUT1 indicates the ability of the spine to engage in glutamate signaling, a key process in memory formation (Riedel *et al.* 2003, Staubli *et al.* 1994). In both cases the proportion of synapsin1 and vGLUT1 was the same between cells treated with vehicle and HFI-419 indicating that these cells have an increased capacity for excitatory synaptic input, a process important for memory formation. Taken together, these data demonstrates that inhibition of IRAP is able to make alterations to dendritic spine structure that may promote lasting changes to memory and learning, and provides evidence for the positive correlation between spine density and learning (O'Malley et al. 1998, Moser et al. 1994, O'Malley et al. 2000, Lai et al. 2012, Fu et al. 2012). However, further studies focusing on the effect of $GLUT_4$ inhibition during HFI-419-mediated memory enhancement *in vivo* are needed to confirm the link between IRAP inhibition, glucose uptake, and memory enhancement.

Conclusion

This study demonstrates that inhibition of IRAP activity with HFI-419 enhances spatial working memory possibly via preferentially enhancing the formation of functional mushroom/stubby spines by facilitating $GLUT_4$-mediated glucose uptake into hippocampal neurons.

Involves human subjects:

If yes: Informed consent & ethics approval achieved:

=> if yes, please ensure that the info "Informed consent was achieved for all subjects, and the experiments were approved by the local ethics committee." is included in the Methods.

ARRIVE guidelines have been followed:
Yes
=> if it is a Review or Editorial, skip complete sentence => if No, include a statement: "ARRIVE guidelines were not followed for the following reason: "
(edit phrasing to form a complete sentence as necessary).
=> if Yes, insert "All experiments were conducted in compliance with the ARRIVE guidelines." unless it is a Review or Editorial

Conflicts of interest: None
=> if 'none', insert "The authors have no conflict of interest to declare."
=> otherwise insert info unless it is already included

Acknowledgements

This work was supported by grants from the Swedish Research Council, the Swedish Brain Foundation, and the Kjell and Märta Beijer Foundation to the Department of Pharmaceutical Biosciences at Uppsala University. Siew Yeen Chai was supported by a National Health and Medical Research Council of Australia, Senior Research Fellowship. The authors also wish to acknowledge that parts of this work have previously appeared in the dissertation of Benjamin John Seyer entitled 'Characterisation of the paradigms used to assess IRAP inhibitors as novel cognitive enhancing agents', Monash University (2017).

Conflict of Interest

The authors declare they have no competing interests.

References

Albiston, A. L., Morton, C. J., Ng, H. L. et al. (2008) Identification and characterization of a new cognitive enhancer based on inhibition of insulin-regulated aminopeptidase. *FASEB J,* **22,** 4209-4217.

Alonso, M., Medina, J. H. and Pozzo-Miller, L. (2004) ERK1/2 activation is necessary for BDNF to increase dendritic spine density in hippocampal CA1 pyramidal neurons. *Learn Mem,* **11,** 172-178.

Benoist, C. C., Wright, J. W., Zhu, M., Appleyard, S. M., Wayman, G. A. and Harding, J. W. (2011) Facilitation of hippocampal synaptogenesis and spatial memory by C-terminal truncated Nle1-angiotensin IV analogs. *J Pharmacol Exp Ther,* **339,** 35-44.

Bosnyak, S., Jones, E. S., Christopoulos, A., Aguilar, M. I., Thomas, W. G. and Widdop, R. E. (2011) Relative affinity of angiotensin peptides and novel ligands at AT1 and AT2 receptors. *Clin Sci (Lond),* **121,** 297-303.

Braszko, J. J., Kupryszewski, G., Witczuk, B. and Wisniewski, K. (1988) Angiotensin II-(3-8)-hexapeptide affects motor activity, performance of passive avoidance and a conditioned avoidance response in rats. *Neuroscience,* **27,** 777-783.

Braszko, J. J., Wlasienko, J., Koziolkiewicz, W., Janecka, A. and Wisniewski, K. (1991) The 3-7 fragment of angiotensin II is probably responsible for its psychoactive properties. *Brain Res,* **542,** 49-54.

Cheng, M., De, B., Pikul, S. et al. (2000) Design and synthesis of piperazine-based matrix metalloproteinase inhibitors. *J Med Chem,* **43,** 369-380.

Dash, P. K., Orsi, S. A. and Moore, A. N. (2006) Spatial memory formation and memory-enhancing effect of glucose involves activation of the tuberous sclerosis complex-Mammalian target of rapamycin pathway. *J Neurosci,* **26,** 8048-8056.

De Bundel, D., Smolders, I., Yang, R., Albiston, A. L., Michotte, Y. and Chai, S. Y. (2009) Angiotensin IV and LVV-haemorphin 7 enhance spatial working memory in rats: effects on hippocampal glucose levels and blood flow. *Neurobiol Learn Mem,* **92,** 19-26.

Diwakarla, S., Nylander, E., Gronbladh, A. et al. (2016a) Binding to and Inhibition of Insulin-Regulated Aminopeptidase by Macrocyclic Disulfides Enhances Spine Density. *Mol Pharmacol,* **89,** 413-424.

Diwakarla, S., Nylander, E., Gronbladh, A. et al. (2016b) Aryl Sulfonamide Inhibitors of Insulin-Regulated Aminopeptidase Enhance Spine Density in Primary Hippocampal Neuron Cultures. *ACS Chem Neurosci,* **7,** 1383-1392.

Fernando, R. N., Albiston, A. L. and Chai, S. Y. (2008) The insulin-regulated aminopeptidase IRAP is colocalised with GLUT4 in the mouse hippocampus--potential role in modulation of glucose uptake in neurones? *Eur J Neurosci,* **28,** 588-598.

Fruitier-Arnaudin, I., Cohen, M., Bordenave, S., Sannier, F. and Piot, J. M. (2002) Comparative effects of angiotensin IV and two hemorphins on angiotensin-converting enzyme activity. *Peptides,* **23,** 1465-1470.

Fu, M., Yu, X., Lu, J. and Zuo, Y. (2012) Repetitive motor learning induces coordinated formation of clustered dendritic spines in vivo. *Nature,* **483,** 92-95.

Garreau, I., Chansel, D., Vandermeersch, S., Fruitier, I., Piot, J. M. and Ardaillou, R. (1998) Hemorphins inhibit angiotensin IV binding and interact with aminopeptidase N. *Peptides,* **19,** 1339-1348.

Gitler, D., Takagishi, Y., Feng, J., Ren, Y., Rodriguiz, R. M., Wetsel, W. C., Greengard, P. and Augustine, G. J. (2004) Different presynaptic roles of synapsins at excitatory and inhibitory synapses. *Journal of Neuroscience,* **24,** 11368-11380.

Hallberg, M., Savmarker, J. and Hallberg, A. (2017) Angiotensin Peptides as AT2 Receptor Agonists. *Curr Protein Pept Sci,* **18,** 809-818.

Jiang, H., Li, J., Katz, E. B. and Charron, M. J. (2001) GLUT4 ablation in mice results in redistribution of IRAP to the plasma membrane. *Biochem Biophys Res Commun,* **284,** 519-525.

Keller, S. R., Davis, A. C. and Clairmont, K. B. (2002) Mice deficient in the insulin-regulated membrane aminopeptidase show substantial decreases in glucose transporter GLUT4 levels but maintain normal glucose homeostasis. *J Biol Chem,* **277,** 17677-17686.

Lai, C. S., Franke, T. F. and Gan, W. B. (2012) Opposite effects of fear conditioning and extinction on dendritic spine remodelling. *Nature,* **483,** 87-91.

Lantz, I., Glamsta, E. L., Talback, L. and Nyberg, F. (1991) Hemorphins derived from hemoglobin have an inhibitory action on angiotensin converting enzyme activity. *FEBS Lett,* **287,** 39-41.

Lee, J., Albiston, A. L., Allen, A. M. et al. (2004) Effect of I.C.V. injection of AT4 receptor ligands, NLE1-angiotensin IV and LVV-hemorphin 7, on spatial learning in rats. *Neuroscience,* **124,** 341-349.

Lee, M. K., Graham, S. N. and Gold, P. E. (1988) Memory enhancement with posttraining intraventricular glucose injections in rats. *Behav Neurosci,* **102,** 591-595.

Mainardi, M., Fusco, S. and Grassi, C. (2015) Modulation of hippocampal neural plasticity by glucose-related signaling. *Neural Plast,* **2015,** 657928.

Moser, M. B., Trommald, M. and Andersen, P. (1994) An increase in dendritic spine density on hippocampal CA1 pyramidal cells following spatial learning in adult rats suggests the formation of new synapses. *Proc Natl Acad Sci U S A,* **91,** 12673-12675.

Murata, H., Hruz, P. W. and Mueckler, M. (2002) Indinavir inhibits the glucose transporter isoform Glut4 at physiologic concentrations. *AIDS,* **16,** 859-863.

Nyberg, G., Sanderson, K., Andren, P., Thornwall, M., Einarsson, M., Danielson, B. and Nyberg, F. (1996) Isolation of haemorphin-related peptides from filter membranes collected in connection with haemofiltration of human subjects. *J Chromatogr A,* **723,** 43-49.

O'Malley, A., O'Connell, C., Murphy, K. J. and Regan, C. M. (2000) Transient spine density increases in the mid-molecular layer of hippocampal dentate gyrus accompany consolidation of a spatial learning task in the rodent. *Neuroscience,* **99,** 229-232.

O'Malley, A., O'Connell, C. and Regan, C. M. (1998) Ultrastructural analysis reveals avoidance conditioning to induce a transient increase in hippocampal dentate spine density in the 6 hour post-training period of consolidation. *Neuroscience,* **87,** 607-613.

Olson, M. L. and Cero, I. J. (2010) Intrahippocampal Norleucine(1)-Angiotensin IV mitigates scopolamine-induced spatial working memory deficits. *Peptides,* **31,** 2209-2215.

Olson, M. L., Olson, E. A., Qualls, J. H., Stratton, J. J., Harding, J. W. and Wright, J. W. (2004) Norleucine1-Angiotensin IV alleviates mecamylamine-induced spatial memory deficits. *Peptides,* **25,** 233-241.

Pederson, E. S., Krishnan, R., Harding, J. W. and Wright, J. W. (2001) A role for the angiotensin AT4 receptor subtype in overcoming scopolamine-induced spatial memory deficits. *Regul Pept,* **102,** 147-156.

Riedel, G., Platt, B. and Micheau, J. (2003) Glutamate receptor function in learning and memory. *Behav Brain Res,* **140,** 1-47.

Rudich, A., Konrad, D., Torok, D. et al. (2003) Indinavir uncovers different contributions of GLUT4 and GLUT1 towards glucose uptake in muscle and fat cells and tissues. *Diabetologia,* **46,** 649-658.

Smith, M. A., Riby, L. M., Eekelen, J. A. and Foster, J. K. (2011) Glucose enhancement of human memory: a comprehensive research review of the glucose memory facilitation effect. *Neurosci Biobehav Rev,* **35,** 770-783.

Staubli, U., Rogers, G. and Lynch, G. (1994) Facilitation of glutamate receptors enhances memory. *Proc Natl Acad Sci U S A,* **91,** 777-781.

Wisniewski, K., Borawska, M. and Car, H. (1993) The effect of angiotensin II and its fragments on post-alcohol impairment of learning and memory. *Pol J Pharmacol,* **45,** 23-29.

Wright, J. W., Clemens, J. A., Panetta, J. A., Smalstig, E. B., Weatherly, L. A., Kramar, E. A., Pederson, E. S., Mungall, B. H. and Harding, J. W. (1996) Effects of LY231617 and angiotensin IV on ischemia-induced deficits in circular water maze and passive avoidance performance in rats. *Brain Res,* **717,** 1-11.

Wright, J. W., Miller-Wing, A. V., Shaffer, M. J., Higginson, C., Wright, D. E., Hanesworth, J. M. and Harding, J. W. (1993) Angiotensin II(3-8) (ANG IV) hippocampal binding: potential role in the facilitation of memory. *Brain Res Bull,* **32,** 497-502.

Wright, J. W., Stubley, L., Pederson, E. S., Kramar, E. A., Hanesworth, J. M. and Harding, J. W. (1999a) Contributions of the brain angiotensin IV-AT4 receptor subtype system to spatial learning. *J Neurosci,* **19,** 3952-3961.

Wright, J. W., Stubley, L., Pederson, E. S., Kramár, E. A., Hanesworth, J. M. and Harding, J. W. (1999b) Contributions of the brain angiotensin IV-AT4 receptor subtype system to spatial learning. *Journal of Neuroscience,* **19,** 3952-3961.

Figure Legends

Figure 1. Time-line of ICV surgery and behavioural studies.

Representative figure showing experimental design and number of animals for each group.

Figure 2. IRAP inhibition with HFI-419 enhanced performance in the SAT.

(A) Rats treated with HFI-419 (0.1 nM; n=8 animals) performed significantly better than those treated with vehicle (10% (v/v) DMSO; p=0.0256; n=8 animals). (B) There was no difference in the number of arm entries between either group, indicating no effect of drug or vehicle administration on locomotor activity. Data were analyzed by two-tailed unpaired t-test. All data are expressed as the mean ± SEM. *p<0.05.

Figure 3. HFI-419 increased total dendritic spine density in hippocampal neurons.

(A) Cultures were exposed to varying concentrations of HFI-419 on 8, 11 and 14 div. At 15 div, hippocampal cells were fixed and immunostained against β-III tubulin (1:500, green) and drebrin (1:500, red) to visualize neuronal processes and dendritic spines, respectively. Images indicate that total spine density is markedly increased when cells are treated with 10^{-6} M (1 μM) HFI-419 compared with vehicle-treated cells. Scale bar = 10 μm. (B) Treatment with HFI-419 produced a bell shaped dose response with respect to total spine density, with a significant effect at 1 μM (p=0.0132). Data represent the mean ± SEM, n = 4 independent cell culture preparations. Data were analyzed by one-way ANOVA followed by post-hoc Dunnet's multiple comparisons test. * p<0.05.

Figure 4. Inhibition of $GLUT_4$ inhibited HFI-419-mediated enhancement of DSD.

Hippocampal cultures were treated with 1 μM HFI-419, which induced a significant increase in total DSD (p=0.0145). However, this increase was abolished by the addition of 50 μM indinavir (I; p=0.0114), which blocks $GLUT_4$-mediated glucose uptake. Dendritic spine density was unaffected by the addition of the MMP-9/MMP-13 inhibitor I (MMP9/13 I) at both doses used (100 and 200 μM). Data represent the mean ± SEM, n = 4 independent cell culture preparations. Data were analyzed by one-way ANOVA followed by post-hoc Dunnet's multiple comparisons against HFI-alone. * p<0.05.

Figure 5. HFI-419 increased glucose uptake in cultured hippocampal neurons, an effect that was blocked by indinavir.

(A) Glucose uptake in cultured hippocampal neurons treated with HFI-419 demonstrated a bell-shaped dose-response with the most effective dose being 10^{-6}M (1μM; $p<0.0200$). (B) Hippocampal neuronal cultures treated with 40 mM K^+ did not exhibit enhanced glucose uptake compared with control, however, treatment with 1 μM HFI-419 produced an approximately 2-fold increase in glucose uptake compared with control and the addition of K^+ did not significantly increase the response further. The addition of 50 μM indinavir abolished the enhanced glucose uptake promoted by HFI-419 treatment alone ($p<0.0438$) and in the presence of K^+ ($p=0.0299$). Data represent the mean ±SEM, n = 5 independent cell culture preparations. Data were analyzed by one-way ANOVA followed by post-hoc Dunnet's multiple comparisons test. * $p<0.05$.

Figure 6. HFI-419 increased total spine density during the peak phase of dendritic growth and the proportion of mushroom/stubby-like spines.

Cultures were exposed to varying concentrations of HFI-419 on 14, 17 and 20 div. At 21 div, hippocampal cells were fixed and immunostained against β-III tubulin (1:500, green) and drebrin (1:500, red) to visualize neuronal processes and dendritic spines, respectively. Nuclei were counterstained with DAPI (blue). (A) Images indicate that total spine density was markedly increased when compared with vehicle-treated cells. Scale bar = 10 μm. Exposure to HFI-419 significantly increased the number of (B) total and (C) stubby/mushroom-like spines at 10^{-6}M (1 μM; $p= 0.0271$ and $p=0.0134$, respectivley) when compared with vehicle control. (D) No change in filopodia/thin-like spines was observed. Brain-derived neurotrophic factor (100 ng/mL) was included as a positive control. Data were analyzed by one-way ANOVA followed by Dunnett's *post hoc* multiple comparisons test. All data are expressed as the mean±SEM, n=3 independent cell culture preparations. * $p<0.05$, ** $p<0.01$ compared with vehicle.

Figure 7. HFI-419 induced the formation of functional dendritic spines.

Cultures were exposed to 10^{-6}M (1 μM) HFI-419 at 14, 17, and 20 div. Spines were labeled for synapsin1 and vGLUT1, and the numbers of spines were counted. With respect to stubby/mushroom-like spines, HFI-419 significantly increased the number of (A) synapsin1-positive spines ($p=0.0129$) and (B) vGLUT1-positive spines ($p=0.0088$) when compared with vehicle-treated cells. However there was no change in the proportion of (C) synapsin-1- or (D) vGLUT-1-positive spines when compared with the total number of (drebrin-positive) spines (p=0.7976 and p=0.3676, respectively). Data were analyzed using an unpaired t-test. All data are expressed as the mean ± SEM, n = 3

independent cell culture preparations. * $p<0.05$ and ** $p<0.01$ compared with vehicle. Scale bar =10 µm.

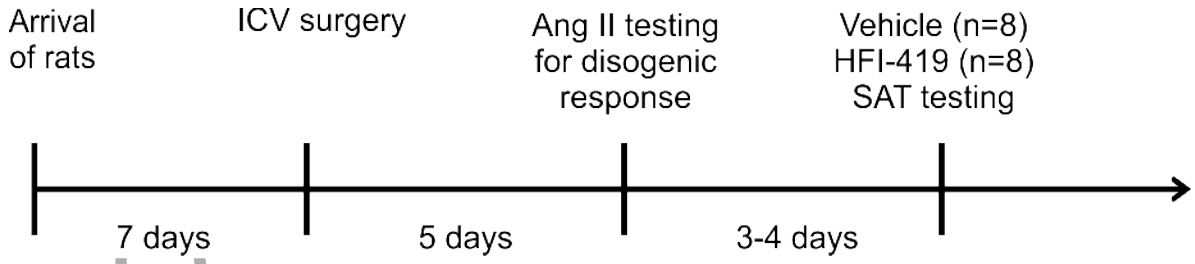

jnc_14880_f1.tif

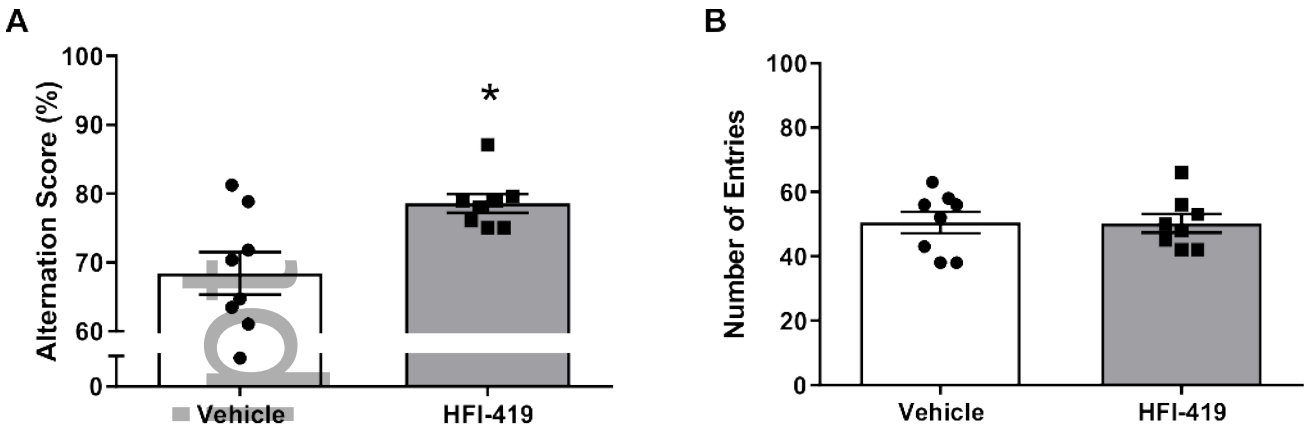

jnc_14880_f2.tif

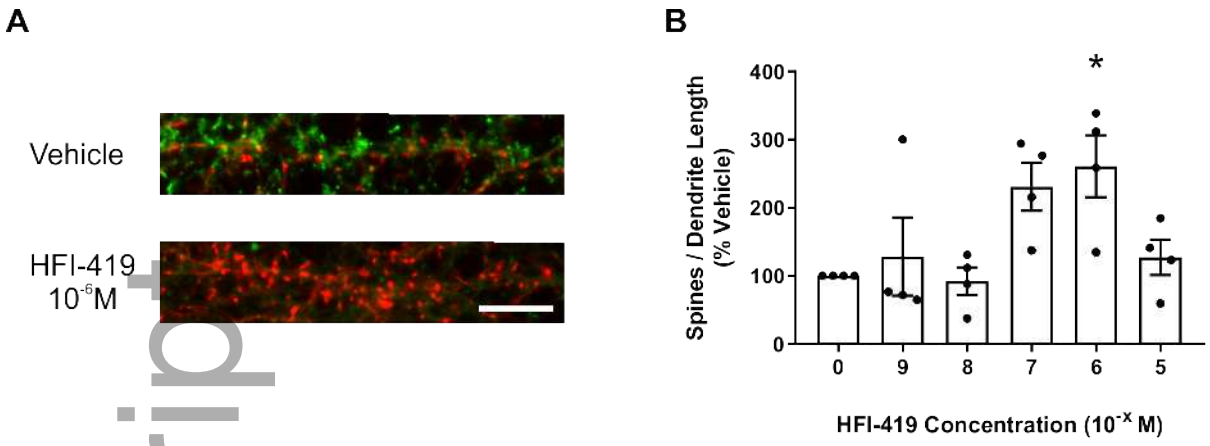

jnc_14880_f3.tif

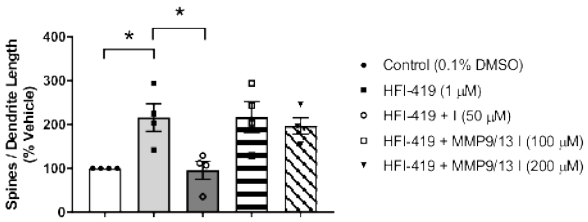

jnc_14880_f4.tif

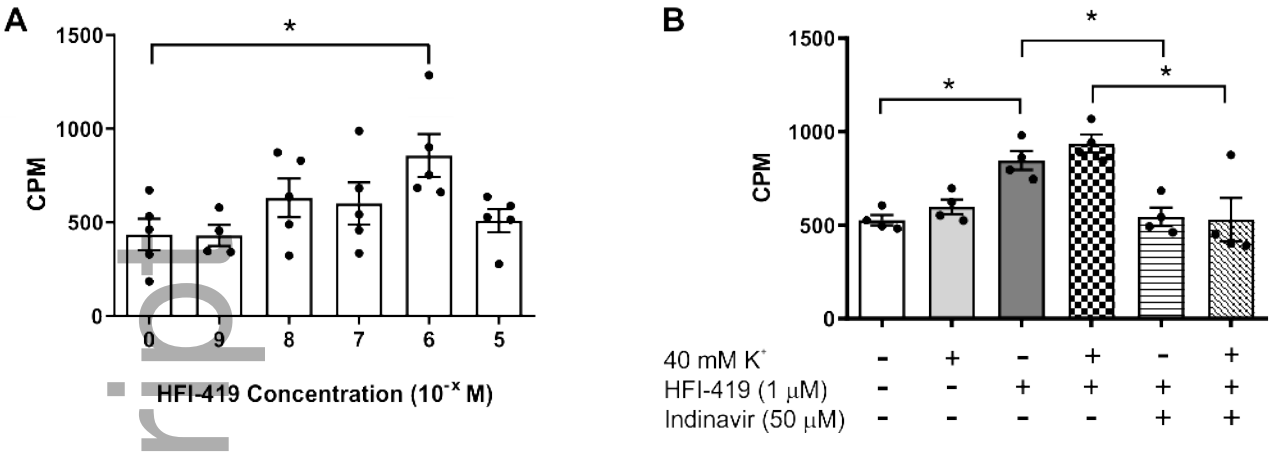

jnc_14880_f5.tif

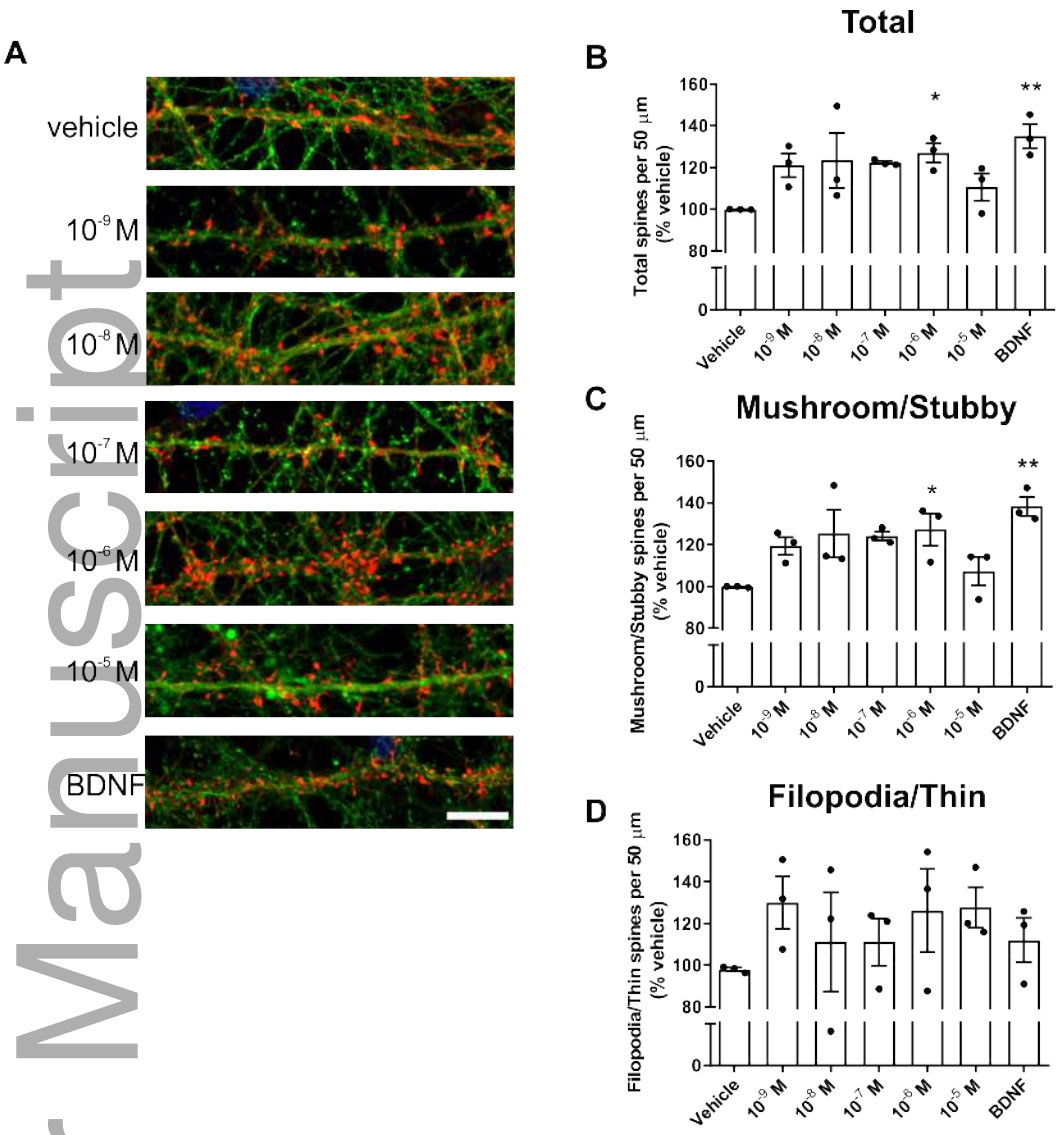

jnc_14880_f6.tif

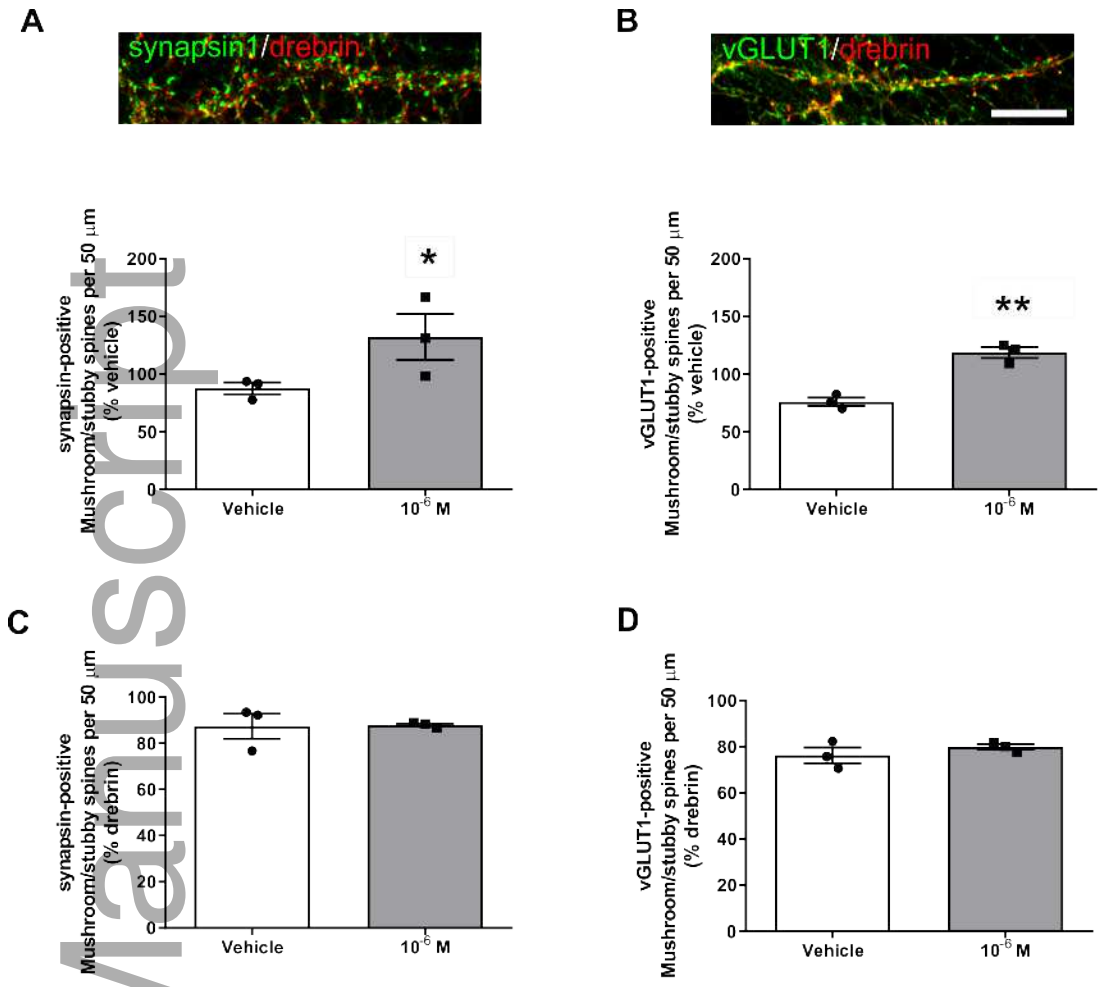

jnc_14880_f7.tif